Journal of Electrical Engineering & Technology (2024) 19:4181–4189
https://doi.org/10.1007/s42835-024-01837-4

ORIGINAL ARTICLE

The Speed Characters of PMSM with Advanced Precise Feedback Linearization Controller

Si-ting Zhou[1] · Jia-qing Ma[1] · Chang-sheng Chen[1] · Tao Qin[1] · Zhi-qin He[1] · Qin-mu Wu[1] · Hong-jv Liu[2] · Yong-jie Li[2]

Received: 19 September 2023 / Revised: 2 January 2024 / Accepted: 25 January 2024 / Published online: 6 March 2024

Abstract

Aiming at the issues of nonlinear strong coupling, low control accuracy, and poor stability of permanent magnet synchronous motor (PMSM), a decoupling model with advanced precise feedback linearization (APFL) of input–output is explored to obtain a more precise speed stabilization effect of the system. The method adopts diffeomorphism transformation and nonlinear system feedback linearization theory to realize the PMSM global decoupling and overall linearized control. The linearized controller with isomorphic mapping between the d-q axis phase currents and the two control inputs is designed by the orthogonal projection method. And from the perspective of the microstructure, the corresponding phase diagram of the experimental results was also drawn to further analyze the system. Simulation and experimental results have demonstrated that the proposed method could accurately achieve the PMSM's expected speed with the advantages of minor overshoot, small static error, high robustness, and strong control accuracy. And the experimental $\Delta n\%$ is less than 5.0% at a high speed in this paper. Therefore, it is available in practical engineering applications.

Keywords Permanent magnet synchronous motor (PMSM) · Feedback · Linearization · Affine nonlinear system · Phase diagram

1 Introduction

Permanent magnet synchronous motors (PMSMs), as the crucial and heart ingredients of complex electromechanical systems, have been comprehensively applied in urban rail vehicles, ship propulsion, high-speed elevators, and wind power generations, because of the strengths of fast dynamic torque response, high overload capability, and wide speed range [1–3]. PMSM is a typical nonlinear control system in that the nonlinear factors are usually ignored when the control accuracy is not demanded. The cascaded proportional-integral (PI) controller can generally tend to address the above problem [4, 5]. However, high precision control is necessarily desired in some areas such as numerical control machine tools and servo systems that the traditional PI control cannot solve the nonlinear characteristics of PMSM and thus the PMSM's nonlinearity elements must be considered to enhance control performance [6].

To attain a more effective analysis and control of the nonlinearity of the PMSM system, some relevant research has been investigated. In [7], Uddin and Lau used the Back-Stepping method for online parametric self-tuning speed control of PMSM, which appropriately demonstrates the system has

✉ Jia-qing Ma
jqma@gzu.edu.cn

Si-ting Zhou
2716889572@qq.com

Chang-sheng Chen
495761009@qq.com

Tao Qin
1147342997@qq.com

Zhi-qin He
641443416@qq.com

Qin-mu Wu
505953130@qq.com

Hong-jv Liu
lhj8233@163.com

Yong-jie Li
yjl20210201@163.com

[1] College of Electrical Engineering, Guizhou University, Guiyang 550025, China

[2] Beijing Jishuitan Hospital Guizhou Hospital, Guiyang 550007, China

good robustness. In [8], nonlinear optimal controller and observer schemes based on a θ-D approximation approach were proposed to averagely solve the problem of controlling the large initial states and excessive online computations. In [9], one improved nonlinear flux observer is studied for sensorless control of PMSM to validly eliminate the issues including dc offset and harmonics compared with the conventional rotor flux estimation method. In [10], a novel nonlinear feedback control based on the dragonfly swarm learning process(D-SLP) algorithm indicates that it can preferably enhance the performance, stability, and robustness of designing the nonlinear system controller. In [11], a novel adaptive super-twisting nonlinear Fractional-order PID sliding mode approach has been achieved to acquire a better speed control performance of PMSM. In [12], a multi-objective integrative control scenario is developed to simultaneously address the load's vibration and torque ripple satisfactorily in a unitary nonlinear control framework. In [13], a method of robust anti-interference control for the angular position tracking control of a PMSM servo system is presented, it could inhibit the influence of uncertain disturbances in the drive control of permanent magnet synchronous machines, containing the parameter uncertainties and load disturbance. In [14], a kind of predictive control (PC) for PMSM control is introduced to achieve more stable and rapid performances as compared to other PCs. And for greatly analyzing the stability and stabilization problem of the nonlinear system of PMSM, an interval type-2 fuzzy-based sampled-data controller for nonlinear systems using novel fuzzy Lyapunov functional has been designed in [15]. For becomingly optimizing the dynamic performance of the PMSM speed regulation system, [16] develops an acceptable nonlinear speed-control algorithm utilizing slide-mode control. In [17], a precise two-axis flux linkage model for PMSMs is proposed to offer a better depiction of the relationship between the flux linkages and corresponding currents for a more exact analysis of saturation and cross-coupling effects that have a significant impact on the magnetic behavior for PMSM. Besides, [18] has studied a methodology, namely the nonlinear finite-element model (FEM), to quantify the effects and assess the relevance of geometric and material uncertainty for performance evaluation on PMSM. In [19], one method utilizing a reverse matrix converter, under variable generator input conditions, has acquired a suitable constant-speed control at low speed for PMSM.

Throughout the above studies, most of them are diffusely concentrated on the control performance optimization of PMSM and simulation analysis, while neglecting the speed ripple when PMSM operates at comparatively high speed and not emphasizing the validation of specific experiments, which has limited its application in high precision position and speed control systems. Therefore, a more appropriate control strategy is urgently demanded to be heightened and the necessity of experimental support is equally valuable. Feedback linearization is a control method for nonlinear systems using a differential geometric framework, which is mainly applied to affine nonlinear systems with feedback linearization. Diffeomorphism transformation and nonlinear state feedback are the core theory of feedback linearization control [20]. It converts algebraic nonlinear system dynamics to linear dynamics, so linear control techniques can be directly applied to nonlinear systems with linearized feedback. Moreover, unlike conventional approximate linearization method (e.g., Jacobi linearization, Taylor series expansion), feedback linearization is achieved through exact state transformations and input–output feedback.

In this article, the most widely used PMSM is taken as the research object, and the input–output precise feedback linearization (PFL [17]) control in nonlinear control theory is adopted as the control strategy to analyze the problem of converting the nonlinear system of PMSM and its converter into a linear system, optimize the corresponding control performance of the system and improve the operation stability of the system [21]. This article is organized as follows. In Sect. 2, the basic model of PMSM is introduced and the affine nonlinear system form of the motor is given. In Sect. 3, the APFL control method is discussed and the corresponding controller is designed. In Sects. 4 and 5, numerical simulation and experimental verification are performed. Finally, Sect. 6 concludes this article.

2 Mathematical Model of PMSM

In the analysis, the following assumptions are adopted: ignoring the leakage flux, disregarding magnetic saturation, eddy current loss, and hysteresis loss, presuming the three-phase symmetry, zero permeability of the permanent magnet material, and sinusoidal distribution of the rotor magnetic chain in the air gap. Then the equation of state for PMSM is as follows [22]:

$$\begin{bmatrix} \dot{i}_d \\ \dot{i}_q \\ \dot{\omega}_r \end{bmatrix} = \begin{bmatrix} -\frac{R_s i_d}{L_d} + \frac{\omega_r L_q i_q}{L_q} \\ \frac{R_s i_q}{L_q} + \frac{\omega_r L_d i_d}{L_q} + \frac{\omega_r \varphi_f}{L_q} \\ \frac{3n_p \varphi_f i_q + 3n_p (L_d - L_q) i_d i_q}{2J} - \frac{T_L}{J} \end{bmatrix} + \begin{bmatrix} \frac{1}{L_d} & 0 \\ 0 & \frac{1}{L_q} \\ 0 & 0 \end{bmatrix} \begin{bmatrix} u_d \\ u_q \end{bmatrix} \quad (1)$$

where u_d, u_q represent the d-axis and q-axis components of the stator voltage; i_d, i_q represent the d-axis and q-axis of the stator current; L_d, L_q represent the d-axis and q-axis elements of the stator inductances; R_s represents the stator resistance; ω_r represents the mechanical angular speed of the rotor; n_p represents the number of pole pairs; J represents the moment of inertia; ψ_f represents the rotor flux; T_L represents the load torque.

In the PMSM system studied in this article: $L_d = L_q = L$ then the Eq. (1) is expressed in the standard form of the affine nonlinear system as follows:

$$\begin{cases} \dot{x} = f(x) + g(x)u \\ y_1 = h_1(x) \\ y_2 = h_2(x) \end{cases} \tag{2}$$

where

$$x = \begin{pmatrix} x_1 \\ x_2 \\ x_3 \end{pmatrix} = \begin{pmatrix} i_d \\ i_q \\ \omega_r \end{pmatrix}, g = \begin{bmatrix} g_1 & 0 \\ 0 & g_2 \\ 0 & 0 \end{bmatrix} = \begin{bmatrix} \frac{1}{L} & 0 \\ 0 & \frac{1}{L} \\ 0 & 0 \end{bmatrix},$$

$$u = \begin{bmatrix} u_d \\ u_q \end{bmatrix}, f(x) = \begin{pmatrix} f_1(x) \\ f_2(x) \\ f_3(x) \end{pmatrix} = \begin{pmatrix} -\frac{R_s i_d}{L} + \omega_r i_q \\ \frac{R_s i_q}{L} + \omega_r i_d + \frac{\omega_r \varphi_f}{L} \\ \frac{3 n_p \varphi_f i_q}{2J} - \frac{T_L}{J} \end{pmatrix}$$

where $h_1(x)$, $h_2(x)$ represent the scalar function.

3 Control Methods of PMSM System

3.1 Traditional PI Controlss

The state-equation of the PMSM in synchronous rotation d-q coordinates is [23–24]

$$\begin{cases} u_d = L\frac{di_d}{dt} + R_s i_d - \omega_e L i_q \\ u_q = L\frac{di_q}{dt} + R_s i_q + \omega_e L i_q + \omega_e \varphi_f \end{cases} \tag{3}$$

where ω_e represents the electric angular speed and $\omega_e = \omega_r n_p$.

From Eq. (3), it can be seen that there exists coupling in the d-q axis voltage, and usually, the coupling term is processed using feedforward compensation, i.e., the PI output is required for coupling offset during PI control. The feedforward compensation voltage [22] is given by

$$\begin{cases} e_d = -\omega_e L i_q \\ e_q = \omega_e L i_d + \omega_e \varphi_f \end{cases} \tag{4}$$

Substituting Eq. (4) into Eq. (3), the feedforward decoupling is

$$\begin{cases} u_d = L\frac{di_d}{dt} + R_s i_d + e_d \\ u_q = L\frac{di_q}{dt} + R_s i_q + e_q \end{cases} \tag{5}$$

The block diagram of SVPWM-based PMSM double-closed-loop PI control can be indicated as shown in Fig. 1.

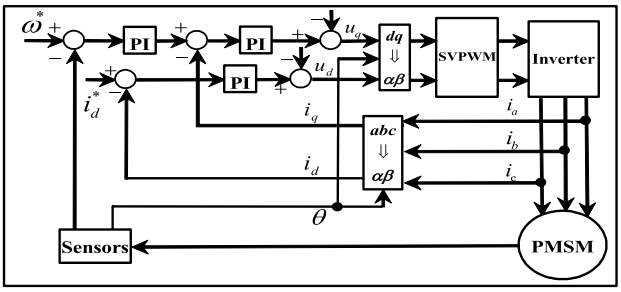

Fig. 1 Block diagram of double closed-loop control of PMSM

3.2 Advanced Precise Feedback Linearization Control of PMSM

To achieve APFL control of PMSM, the affine nonlinear mathematical model of PMSM is employed to complete the linearization theory. The specific implementation is to design the controller on a mathematical model with linearized feedback. In this section, the input–output feedback of PMSM is linearized by adequate feedback transformations, thus converting the complex nonlinear system synthesis problem into a comprehensively linear solution.

From Eqs. (1) and (2), we know that

$$\begin{cases} \dot{i}_d = -\frac{R_s i_d}{L} + \omega_r i_q + \frac{u_d}{L} \\ \dot{\omega}_r = \frac{3 n_p \varphi_f i_q}{2J} - \frac{T_L}{J} \end{cases} \tag{6}$$

Since does not contain the actual control quantity, we perform a second-order derivative of ω_r to obtain

$$\ddot{\omega}_r = \frac{3 n_p \varphi_f}{2J}\dot{i}_q - \frac{\dot{T}_L}{J} = \frac{3 n_p \varphi_f}{2JL}\left(R_s i_q + L\omega_r i_d + \omega_r \varphi_f + u_q\right) - \frac{\dot{T}_L}{J} \tag{7}$$

At this point, a new pair of linear control input is introduced. According to Eqs. (6) and (7), we get

$$\begin{cases} u_d = L\left(v_1 + \frac{R_s i_d}{L} - \omega_r i_q\right) \\ u_q = \frac{2JL}{3 n_p \varphi_f}\left(v_2 + \frac{\dot{T}_L}{J}\right) - R_s i_q - L\omega_r i_d - \omega_r \varphi_f \end{cases} \tag{8}$$

where $v_1 = \dot{i}_d$, $v_2 = \ddot{\omega}_r$.

After the PFL of the PMSM is completed, the controller design can be performed according to the classical linear control principle and Eq. (8). This article designs the controller by adopting the pole configuration method. Assuming that providing a controlled system, then its state feedback law is

$$u = -Kx + \gamma \tag{9}$$

where $\boldsymbol{\gamma}$ is the input quantity of reference value, and $\boldsymbol{K}$ is the status feedback gain matrix. Equation (9) can satisfy the following equation of state

$$x = (A - BK)x + Bu \tag{10}$$

where matrix $\boldsymbol{A}=f(x)$, $B=f(x)$ the poles are $\{\lambda_1^*, \lambda_2^*, \lambda_3^*, \ldots \lambda_n^*\}$. In turn, the following equation can be derived

$$\lambda_i = (A - BK) = \lambda_i^* i = 1, 2, \ldots, n \tag{11}$$

Therefore, there exists $v_1 = i_d = -k_1 i_d + \alpha i_d^*$. The coefficients $\alpha = k_1$, $k_1 = 1/T_0$ are obtained from the definition of the closed-loop transfer function of the first order. So we have the following equation

$$\begin{cases} v_1 = -k_1 i_d + k_1 i_d^* = k_1\left(i_d^* - i_d\right) \\ v_2 = -k_2\omega_r - k_3\dot{\omega}_r + \beta\omega_r^* = k_2\left(\omega_r^* - \omega_r\right) - k_3\dot{\omega}_r \end{cases} \tag{12}$$

To acquire a fast response, the system regulation time is taken to be a smaller value, i.e. $t_s = 2\ ms$, From the knowledge of the automatic control principle, $t_s = 3.5T_0$, thus $T_0 = 4/7\ ms$.

Similarly, $\beta = k_2 = \omega_n^2$, $k_3 = 2\xi\omega_n$ is obtained. Taking the damping ratio, $\xi = 0.707$, $t_s' = 10t_s$, and owing to $t_s' = 3.5/\xi\omega_n$, thus $\xi\omega_n = 175$. Correspondingly, the undamped natural frequency $\omega_n \approx 247.53$, and $k_2 = \omega_n^2 = 61{,}271$, $k_3 = 2\xi\omega_n = 350$, we get

$$\begin{cases} v_1 = 1750\left(i_d^* - i_d\right) \\ v_2 = 61271\left(\omega_r^* - \omega_r\right) - 350\,\dot{\omega}_r \end{cases} \tag{13}$$

Equations (13) and the values of each parameter are substituted into Eq. (11). Since the values of some terms are very small and have little impact on the whole system, after simplification with $i_d^* = 0$, Eq. (8) turns out to be a simplified one with APFL.

$$\begin{cases} u_d = -1750Li_d \\ u_q = 61271 \cdot \frac{2JL}{3n_p\varphi_f}\left(\omega_r^* - \omega_r\right) \end{cases} \tag{14}$$

The APFL control block diagram of PMSM is shown in Fig. 2.

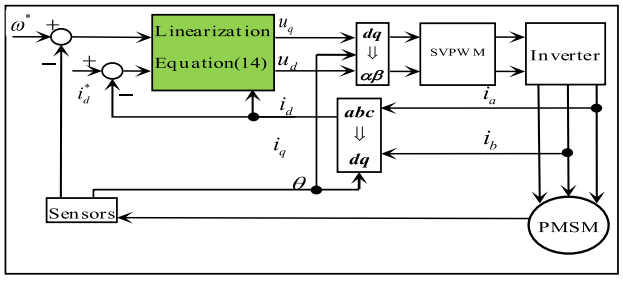

Fig. 2 The APFL control block diagram of PMSM

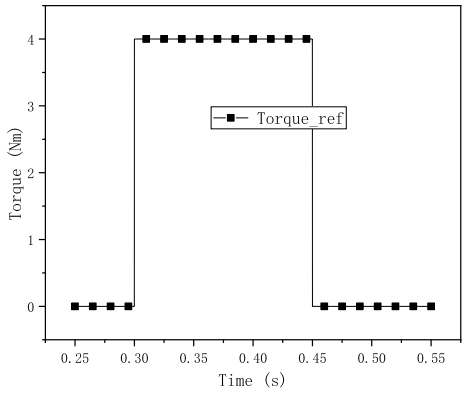

Fig. 3 The input of torque load

4 Simulation and Analysis of Results

In an attempt to verify the effectiveness of the above theoretical control, the PI control method based on SVPWM and the proposed PFL control were respectively used for comparison. Simulation models were built in Matlab/Simulink for both control systems.

Meanwhile, the identical speed command is set to ensure PI control and PFL control simulation runs under the equivalent conditions. Figure 3 shows the same load torque input for the PMSM system for both PFL control and APFL control. Figure 4(a) and 4(b) show the speed tracking process of PMSM under these two controls, which presents a slower rise-time because of the existence of the differential term in Eq. (14) under APFL control.

Under the input load torque shown in Fig. 3, the output magnitude of electromagnetic torque in the two approaches is shown in Figs.4(c) and (d). It can be revealed that the output torque fluctuation of feedback linearized control is narrower than PFL controller, the efficiency of torque regulation is increased, and the motor control performance is well improved.

Moreover, selecting one cycle that is after 0.30 s, the FFT analysis of the A-phase current at a carrier frequency of 20 kHz and a fundamental frequency of 100 Hz is performed. The results are shown in Figs.5, which have represented that the THD (total harmonic distortion) of PFL control and APFL control is 52.00% and 39.08%, respectively, thus the THD of APFL control is reduced. Through the simulation results' analysis, it can be known that the APFL control has good control performance.

5 Experiments and Analysis of Results

This section presents experimental verification of the PMSM control system based on APFL of input–output the experimental platform is depicted in Fig. 6.

Fig. 4 Rotating speed and electromagnetic torque of PMSM under inputting load. **a**The load is 4N•m when nref = 1120r/min. **b** The load is 8N•m when nref = 1120r/min. **c** The load is 4N•m when nref = 1618r/min. **d** The load is 8N•m when nref = 1618r/min

First, the low-medium speed experiment was conducted, and the torque is taken as disturbance and the load torque is selected as 4 N·m and 8 N·m, and its effect on the motor speed and current is shown in Fig. 7.The $\Delta n\%$ is the error of the control speed. Although 8 N·m exceeds the maximum load torque of the motor, the excess is small and the time is short, which is significant to examine the stability of the motor with APFL control. Figure 7(a) shows the $\Delta n\%$ is 4.20% for a load torque of 4 N·m, and Fig. 7(b) shows the $\Delta n\%$ is 12.50% for a load torque of 8 N·m.

Second, based on the above, to test the control effect of the proposed APFL control method at higher speeds, experiments were conducted at the measured currents of 1618r/min and 1835r/min to observe the stability of the speeds. The PMSM speed and current variation are respectively displayed in Fig. 8, in which input load torque is 4 N·m (the input torque inertia of 8 N·m is removed in this case). From Fig. 8, it can be seen that the $\Delta n\%$ is 4.64% at a speed of 1618 r/min, and the $\Delta n\%$ is 4.90% at a speed of 1835 r/min.

Then we analyze the experimental results from a microscopic perspective. Firstly, the three-phase stationary coordinate system is transformed into a two-phase rotating coordinate system by Clark transform and Park transforms, that is, the current i_a, i_b, i_c is changed into i_d, i_q, and the speed n is changed into ω, where ω is the electrical rotor angular speed. After that, the system time-domain diagram and phase diagram are drawn, taking Fig. 7(a) and Fig. 8(b) as examples. From Fig. 9 and Fig. 10, it can be seen that before and after adding the load torque, when the motor is running at low-medium speed and higher speed, the variables all always move irregularly within a certain range around two stable speed points [25]. The above content reflects the effectiveness of APFL control in PMSM.

s show that the $\Delta n\%$ of PMSM at 1120 r/min are 4.20% and 12.50%, respectively. When the input load torque is 4 N·m, the experimental results show that the $\Delta n\%$ of PMSM at 1618 r/min and 1835 r/min are 4.64% and 4.90%, respectively. In addition, the three-dimensional phase diagram also shows that the entire trajectory of the variables is within a certain range. Through the above experimental results' analysis, it can be known that the APFL control achieves a better control effect.

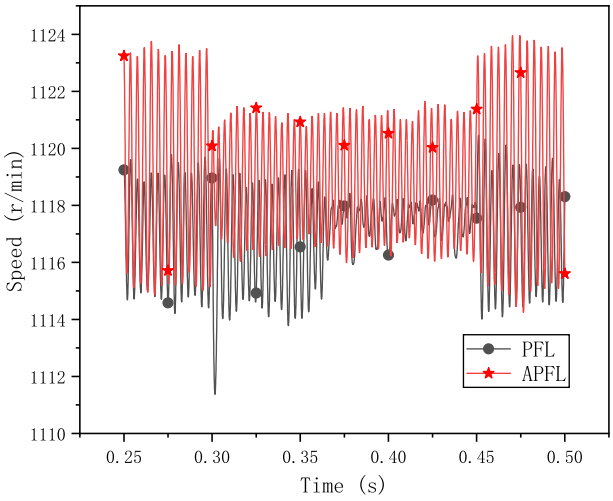

(a)The load is 4N•m when nref=1120r/min.

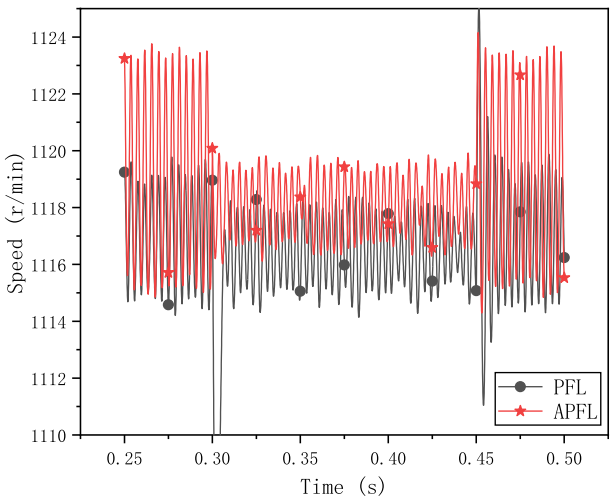

(b) The load is 8N•m when nref=1120r/min.

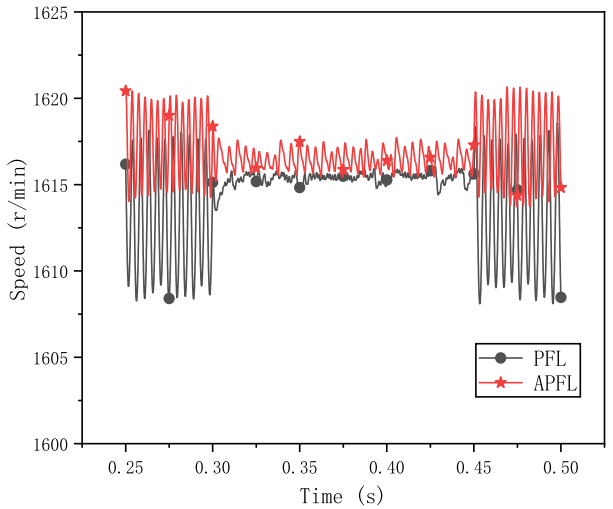

(c) The load is 4N•m when nref=1618r/min.

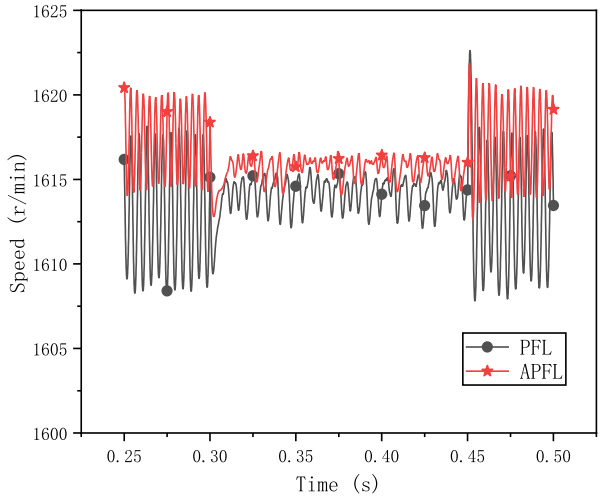

(d) The load is 8N•m when nref=1618r/min.

Fig. 4 (continued)

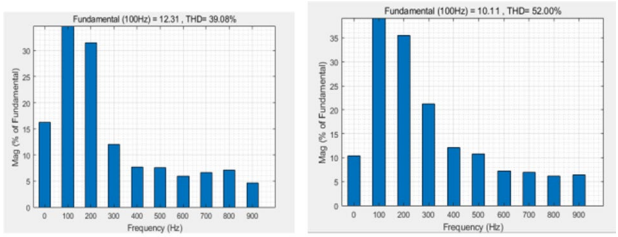

(a) The THD of PFL controller (b) The THD of APFL controller.

Fig. 5 FFT analysis of phase current in PMSM. **a** The THD of PFL controller **b** The THD of APFL controller

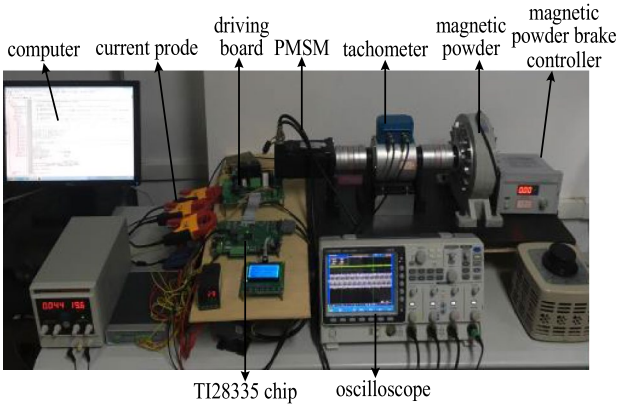

Fig. 6 The experimental platform of PMSM

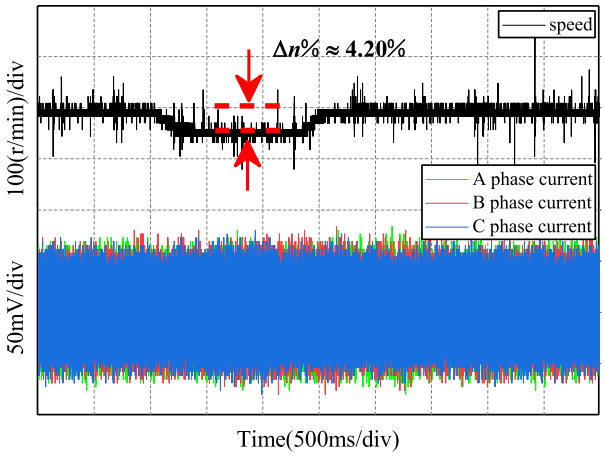

(a)Input load torque of 4 N·m(1120 r/min)

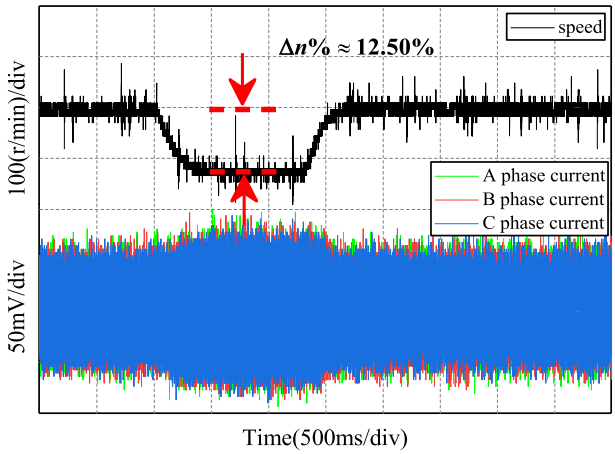

(b)Input load torque of 8 N·m(1120 r/min)

Fig. 7 Speed test of input load torque for PMSM. **a** Input load torque of 4 N·m(1120 r/min). **b** Input load torque of 8 N·m(1120 r/min)

6 Conclusion

In this article, the APFL strategy of input and output is improved to obtain a more accurate speed tracking effect for the shortcomings of low control accuracy and poor stability of the traditional control method of PMSM. Furthermore, The APFL with differential homeomorphism transformation and nonlinear system feedback linearization is simplified on the basis of PFL. Simulation and experiment show that the APFL effectively improves the speed stability and speed control accuracy of PMSM with drawing the corresponding phase diagram. It is proved that the APFL control method is more effective than the PFL control. It also can ensure

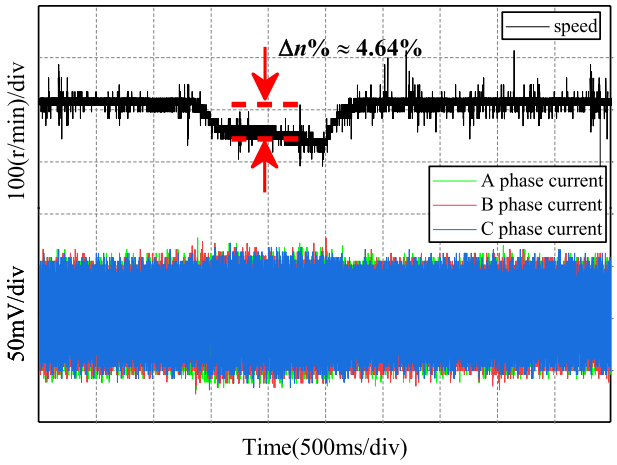

(a) Input load torque of 4 N·m (1618 r/min)

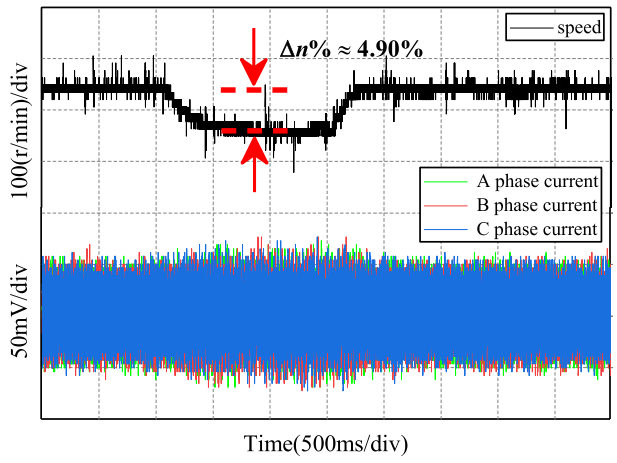

(b) Input load torque of 4 N·m (1835 r/min)

Fig. 8 Speed test of input load torque for comparatively high speed of PMSM. **a** Input load torque of 4 N·m (1618 r/min). **b** Input load torque of 4 N·m (1835 r/min)

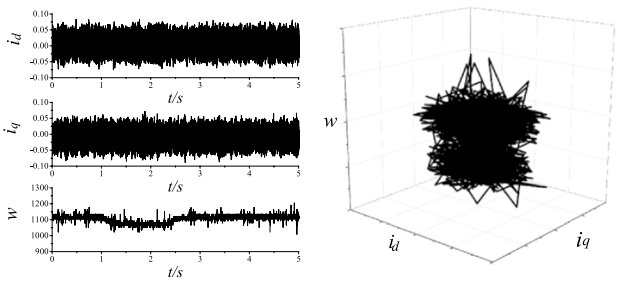

(a)Time-domain diagram (b) Phase diagram of id-iq-ω

Fig. 9 Time-domain diagram and three-dimensional phase diagram of Fig. 7(a). **a**Time-domain diagram. **b** Phase diagram of id-iq-ω

stable speed tracking even when the motor is running at a higher speed. The control performance of PMSM is also improved with the advantages of small static error, strong

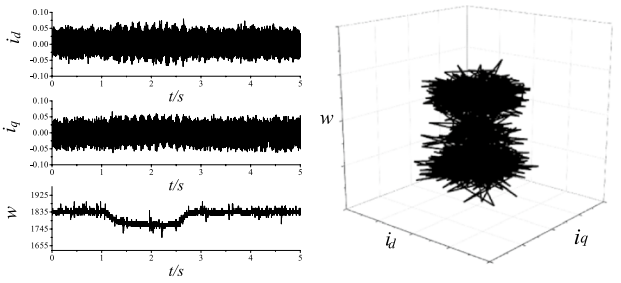

(a)Time-domain diagram (b) Phase diagram of id-iq-ω

Fig. 10 Time-domain diagram and three-dimensional phase diagram in Fig. 8(b). **a**Time-domain diagram. **b** Phase diagram of id-iq-ω

robustness and high control accuracy when the APFL is adopted. Meanwhile, the treatment of differential terms, disturbance terms, and viscosity coefficients of the PMSM system will be deeply studied in the future to further optimize the performance of input–output APFL control for PMSM. In conclusion, the modified APFL control for PMSM has excellent dynamicity and stability.

Acknowledgements This work was supported by the National Natural Science Foundation of China (62163006), and Guizhou provincial science and technology department(PGTS[2021]G442,[2022]G244,[2023]G096,[2023]G179).

Declarations

Conflict of interest The authors declare that they have no known competing financial interests or personal relationships that could have appeared to influence the work reported in this paper.

References

1. Li T, Sun X, Lei G, Yang Z, Guo Y, Zhu J (2022) Finite-control-set model predictive control of permanent magnet synchronous motor drive systems—an overview. IEEE/CAA J Autom Sin 9(12):2087–2105
2. Uddin MN, Lau J (2004) Adaptive backstepping based nonlinear control of an IPMSM drive. IEEE PESC 5:3451–3457
3. T. Li, X. Sun, M. Yao, D. Guo, and Y. Sun (2023). Improved finite control set model predictive current control for permanent magnet synchronous motor with sliding mode observer. IEEE Trans. Transport. Electrific.
4. Sun X, Zhang Y, Cai Y, Tian X (2022) Compensated deadbeat predictive current control considering disturbance and VSI nonlinearity for in-wheel PMSMs. IEEE/ASME Trans Mechatronics 27(5):3536–3547
5. Do TD, Choi HH, Jung JW (2015) θ-D approximation technique for nonlinear optimal speed control design of surface-mounted PMSM drives. IEEE/ASME Trans Mechatron 20(4):1822–1831
6. Sun X, Xu N, Yao M, Cai F, Wu M (2023) Efficient feedback linearization control for an IPMSM of EVs based on improved firefly algorithm. ISA Trans 134:431–441
7. Gao P, Zhang G, Ouyang H, Mei L (2020) An adaptive super twisting nonlinear fractional order PID sliding mode control of

permanent magnet synchronous motor speed regulation system based on extended state observer. IEEE Access 8:53498–53510
8. Yu Y et al (2020) A stator current vector orientation based multi-objective integrative suppressions of flexible load vibration and torque ripple for PMSM considering electrical loss. CES Trans Electr Mach Syst 4(3):161–171
9. Li L et al (2020) Robust position anti-interference control for PMSM servo system with uncertain disturbance. CES Trans Electr Mach Syst 4(2):151–160
10. Wei Y, Wei Y, Sun Y, Qi H, Guo X (2020) Prediction horizons optimized nonlinear predictive control for permanent magnet synchronous motor position system. IEEE Trans Ind Electron 67(11):9153–9163
11. Shanmugam L, Joo YH (2021) Design of interval type-2 fuzzy-based sampled-data controller for nonlinear systems using novel fuzzy lyapunov functional and its application to PMSM. IEEE Trans Syst Man Cybern Syst 51(1):542–551
12. Wang Y, Feng Y, Zhang X, Liang J (2020) A new reaching law for antidisturbance sliding-mode control of PMSM speed regulation system. IEEE Trans Power Electron 35(4):4117–4126
13. Sun X, Xiao X (2020) Precise non-linear flux linkage model for-permanent magnet synchronous motorsbased on current injection and bivariatefunction approximation. IET Electr Power Appl 14(11):2044–2050
14. Beltrán-Pulido A, Aliprantis D, Bilionis I, Munoz AR, Leonardi F, Avery SM (2020) Uncertainty quantification and sensitivity analysis in a nonlinear finite-element model of a permanent magnet synchronous machine. IEEE Trans Energy Convers 35(4):2152–2161
15. Bak Y, Lee KB (2018) Constant speed control of a permanent-magnet synchronous motor using a reverse matrix converter under variable generator input conditions, IEEE. J Emerg Sel Top Power Electron 6(1):315–326
16. Wang XX, Ding G, Han ZJ (1999) H∞ control approach for induction motors based on the feedback linearization[J]. Control Decis 14(5):413–417
17. Chaojiang Y, Jiaqing Ma (2019) Research on low speed operation characteristics of permanent magnet synchronous motor based on accurate feedback linearization control[J]. Electr Mach Control Appl 46(06):1–748
18. Ping Z, Wang T, Huang Y, Wang H, Lu JG, Li Y (2020) Internal model control of PMSM position servo system: theory and experimental results. IEEE Trans Ind Inf 16(4):2202–2211
19. Badini SS, Verma V (2020) A new stator resistance estimation technique for vector-controlled PMSM drive. IEEE Trans Ind Appl 56(6):6536–6545
20. Zhang R, Yin Z, Du N, Liu J, Tong X (2021) Robust adaptive current control of a 1.2-MW direct-drive PMSM for traction drives based on internal model control with disturbance observer. IEEE Trans Transp Electrif 7(3):1466–1481
21. Li Z, Park JB, Joo YH, Zhang B, Chen G (2002) Bifurcations and chaos in a permanent-magnet synchronous motor. IEEE Trans Circuits Syst I, Fundam Theory Appl 49(3):383–387

Si-ting Zhou She received her B.S. degree in automation from Guizhou University. She is pursuing a master's degree in control science and engineering at Guizhou University. She is interested in precise feedback linearization control.

Jia-qing Ma He received his B.Sc. degree in 2008 from Sichuan Normal University , received his Ph.D. degree in 2014 from Xinan Jiaotong University, now he is an associate professor in Guizhou University. His main research interests include the intelligent controller of AC Motor and thenonlinear control of power electronics.

Chang-sheng Chen He received his Master Degree in Engineering in 2014 from Guizhou University, and now he is a senior experimentalist at Guizhou University. His main research interests include the Industrial Robot and Embedded.

Tao Qin He received his master degree in 2018 from Guizhou University and now he is a lecturer at Guizhou University. His main research interests include Embedded AI computing and smart IoT system.

Zhi-qin He She received her B.S. degree in 2005 from Guizhou University, now she is a professor at Guizhou University. Her main research interests include the intelligent controller of AC Motors and the nonlinear control of power electronics.

Qin-mu Wu He received the B.S. degree in automation and the M.S. degree in control science and engineering from the Guizhou University of Technology, in 2001, and the Ph.D. degree in control science and engineering from the Huazhong University of Science and Technology, Wuhan, China. He is currently a Professor and a Ph.D. Supervisor with the College of Electrical Engineering, Guizhou University. His current research interests include control theory and applications, networked control, electric vehicle transmission control, and deep learning.

Hong-jv Liu He received his B.M degree in 2004 from Guizhou Medical University, received his M.D. degree in 2019 from Capital Medical University, now he is a Chief Physician in Beijing Jishuitan Hospital Guizhou Hospital.His main research direction is prevention and treatment of musculoskeletal diseases.

Yong-jie Li He received his B.S degree in 2018 from Shanxi University of Traditional Chinese Medicine, received his M.E. degree in 2021 from Wuhan Sports University, now he is a physiatrist in Beijing Jishuitan Hospital Guizhou Hospital. His main research direction is prevention and treatment of musculoskeletal diseases.